

Article

Preparation of Thermally Conductive Silicone Rubber-Based Ultra-Thin Sheets with Low Thermal Resistance and High Mechanical Properties

Mengqi Liu ^{1,2,3}, Shengfu Tong ⁴, Xinhua Guo ^{1,2}, Jing Ye ¹, Jianping Liu ^{1,3,*} and Chenlu Bao ^{1,2,3,*}

¹ School of Material Science and Engineering, Tiangong University, 399 Binshui West Road, Tianjin 300387, China

² Tianjin HaiTe Thermal Management Technology Co., Ltd., 6 Huake Eight Road, Tianjin 300450, China

³ Sichuan Ximaiwan Technology Co., Ltd., 6668 Section 2 Qingquan Avenue, Chengdu 610300, China

⁴ Zhejiang Public Information Industry Co., Ltd., A3-3, China Telecom Zhejiang Innovation Park, 8 Xiqin Street, Hangzhou 311100, China

* Correspondence: liujianpinglj@tiangong.edu.cn (J.L.); baocl@mail.ustc.edu.cn (C.B.)

Abstract: Thermally conductive silicone rubber (TCSR)-based thin sheets with low thermal resistance and high electrical insulation properties have been widely used in thermal management applications in the electronic and energy storage fields. The low thermal resistance is mainly attributed to the sheets' small thickness. In order to further decrease the sheets' thermal resistance, it is necessary to decrease their thickness. However, the sheets mostly have a thickness of at least 0.20 mm, and it is still a challenge to decrease the thickness to less than 0.10 mm mainly due to the difficulty of smooth calendaring through a narrow roll-to-roll gap on calenders. Here, a low-viscosity calendaring method has been developed to prepare TCSR-based ultra-thin sheets. The sheets present unprecedentedly small thickness (~0.08 mm), low thermal resistance (0.87 cm²K/W), high tensile strength (~8 MPa), high flexibility, high electrical resistance (>10¹⁴ Ω·cm), and high thermal dissipation (>30 °C decrease in LED working temperature). Comparison studies between this new method and the conventional preparation method have been carried out to understand the mechanism of the improvements.

Keywords: thermally conductive silicone rubber; thin sheets; thermal resistance; calendaring process; thermal dissipation



Citation: Liu, M.; Tong, S.; Guo, X.; Ye, J.; Liu, J.; Bao, C. Preparation of Thermally Conductive Silicone Rubber-Based Ultra-Thin Sheets with Low Thermal Resistance and High Mechanical Properties. *Processes* **2023**, *11*, 1184. <https://doi.org/10.3390/pr11041184>

Academic Editor: Heon E. Park

Received: 7 February 2023

Revised: 26 February 2023

Accepted: 28 February 2023

Published: 12 April 2023



Copyright: © 2023 by the authors. Licensee MDPI, Basel, Switzerland. This article is an open access article distributed under the terms and conditions of the Creative Commons Attribution (CC BY) license (<https://creativecommons.org/licenses/by/4.0/>).

1. Introduction

The rapid development of electronic and energy storage devices has brought increasing demand for high-performance thermal interface materials (TIMs) to reduce thermal resistance in their thermal management systems [1–3]. TIMs such as thermally conductive grease, thermally conductive silicone rubber (SR) sheets, and thermally conductive structural adhesives have taken important roles in their thermal management systems. Low thermal resistance is of great importance for TIM applications. In recent years, a range of highly thermally conductive thin sheets, such as graphene films, boron nitride (BN) papers, carbon fiber-based films, and MXene films that have extremely high thermal conductivity and low thermal resistance have gained great research interest [4–10]. They have been regarded as a new generation of high-performance TIMs. However, their potential in practical applications has been limited by various factors such as low electrical insulation properties (graphene and MXene are conductors), lack of industrial-scale production techniques, and high cost.

In comparison, thermally conductive silicone rubber (SR) (TCSR)-based thin sheets, which are also known as thermally conductive insulators in the industry, have been widely used in practical applications, although they have higher thermal resistance and lower thermal conductivity than most of the thin sheets mentioned above. TCSR-based thin sheets

are usually composed of silicone rubber, glass fabrics (GFs), and thermally conductive fillers such as alumina or aluminum hydroxide. Silicone rubber and thermally conductive fillers make up thermally conductive silicone rubber, which is coated on the surface of the glass fabric. TCSR-based thin sheets usually have low thermal resistance, high electrical insulation properties, high breaking voltage, high mechanical properties, sufficient industrial production capacity, and low cost. These advantages make TCSR-based thin sheets promising in a wide range of applications such as power switches, insulated gate bipolar transistors, batteries, and radio frequency devices. However, although TCSR-based thin sheets are popular in practical applications, the fast development of other low thermal resistance TIMs has brought great pressure of competition to TCSR-based thin sheets. It has become urgent for TCSR-based thin sheets to further decrease their thermal resistance.

The thermal resistance of TIMs is generally proportional to their thickness and inversely proportional to their thermal conductivity [11–14]. The thermal conductivity of TCSR-based thin sheets is usually not high. For instance, most of them have a thermal conductivity of less than 5 W/mK. In comparison, the thermal conductivity of neat TCSR can reach 15 W/mK or even higher. Therefore, TCSR-based thin sheets' low thermal resistance is mainly attributed to their small thickness. If the thickness can be effectively decreased, it is possible to develop TCSR-based thin sheets with extremely low thermal resistance. Currently, the thickness is mostly at least 0.20 mm, and it is still a challenge to decrease the thickness to less than 0.10 mm (there is no open literature for these data, and the authors know the data because they have run companies producing TIMs). This challenge can be mainly attributed to the production process of TCSR-based thin sheets. The sheets are mostly prepared on a calender, which presses raw material fluids into thin sheets through a roll-to-roll narrow gap (usually <0.50 mm) in a continuous manner. The sheets' thickness is controlled by the size of the gap. In order to decrease the sheets' thickness, the gap must be narrow enough. However, a narrow gap may bring greatly increased flow resistance to raw material fluids, making the calendaring process difficult.

In order to overcome this challenge, it is necessary to reduce the viscosity of the raw material fluids. The high viscosity is mainly caused by the high viscosity of the liquid raw materials, the high loading level of thermally conductive fillers, and a combination effect of the fillers' shape, size, components, etc. The viscosity can be reduced by three main methods, (i) decreasing thermally conductive fillers' loading level in the fluids; (ii) optimizing the multi-sizes synergism effect between fillers; and (iii) reducing the viscosity of silicone oil. As has been shown by a number of studies, decreasing the fillers' loading level (method i) usually brings decreased thermal conductivity, which will cause increased thermal resistance in the final composites [2,13,15–17]. Therefore, the latter two methods are more feasible.

In this contribution, a low-viscosity calendaring method has been developed to produce TCSR-based ultra-thin sheets (Figure 1). Fine spherical alumina and low-viscosity silicone oil have been used to reduce the viscosity of the raw material fluids and hence promote smooth calendaring. Comparison studies between this new method and the conventional method have been carried out to understand the mechanism of the improvements.

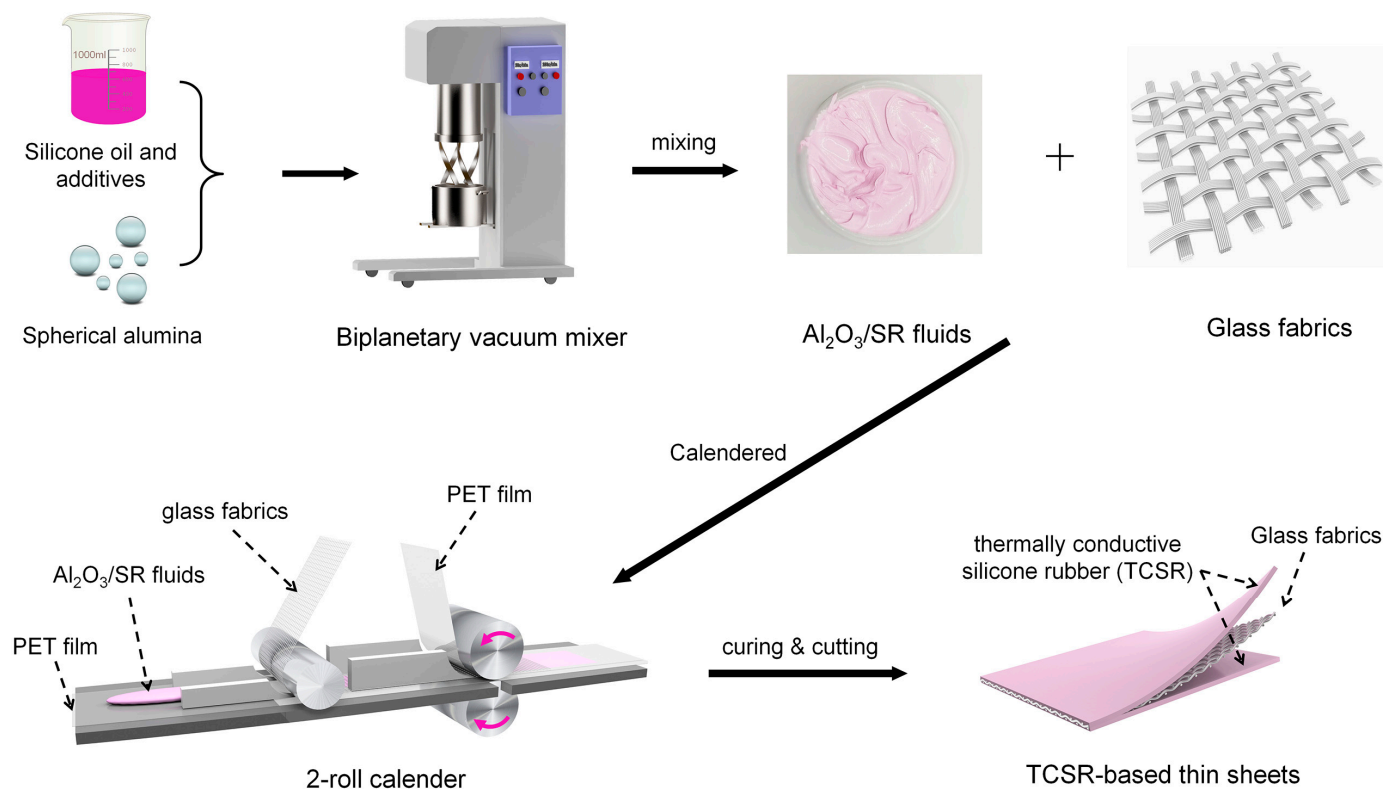


Figure 1. Schematic diagram of the preparation process of TCSR-based thin sheets.

2. Materials and Methods

2.1. Materials

Spherical alumina (powders, mean size of 2, 5, 10, or 20 μm) were purchased from Jiangsu Lianrui New Materials Co., Ltd., Lianyungang, Jiangsu Province, China. Vinyl silicone oil (viscosity of 500 or 100 $\text{mPa}\cdot\text{s}$), double-end-hydrogen silicone oil (hydrogen concentration of 0.11–0.13 wt.%), and side-hydrogen silicone oil (hydrogen concentration of 0.75–0.79 wt.%) were purchased from Zhejiang Runhe Organosilicone New Material Co., Ltd., Ningbo, Zhejiang Province, China. Platinum (Pt) catalyst and inhibitor were bought from Dongguan Huachun Organic Silicon Material Co., Ltd., Dongguan, Guangdong Province, China. Color masterbatches (blue and red) were purchased from Dongguan City Shenglibao Organosilicon Technology Co., Ltd., Dongguan, Guangdong Province, China. Dodecyl trimethyl siloxane (DTMS) was purchased from Hubei Jusheng Technology Co., Ltd., Tianmen, Hubei Province, China. Glass fabrics (thickness 40 μm) were purchased from Renqiu Boda Industry and Trade Co., Ltd., Renqiu, Hebei Province, China. PET films were purchased from Dongguan Dingli Film Technology Co., Ltd., Dongguan, Guangdong Province, China. Kapton PI film (0.05 mm thick, produced by DuPont, Wilmington, DE, USA) and thermally conductive grease (X-23-7783D, produced by ShinEtsu, Japan) were purchased on www.taobao.com (accessed on 10 September 2021). Thermally conductive silicone rubber pads with high thermal conductivity (5 W/mK and 7 W/mK) were kindly provided by Tianjin Haite Thermal Management Technology Co. Ltd., Tianjin, China). All materials were used as received.

2.2. Preparation of TCSR-Based Thin Sheets by the Conventional Method

In the industrial production of TCSR-based thin sheets, spherical alumina powders (mean size of 5–30 μm) are the most widely used thermally conductive fillers, and vinyl silicone oil with a viscosity of 500–1000 $\text{mPa}\cdot\text{s}$ is the most widely used silicone oil. Here we prepared TCSR-based thin sheets from these raw materials by the conventional method for comparison studies.

Vinyl silicone oil (500 mPa·s), side-hydrogen silicone oil, Pt catalyst, inhibitor, color masterbatch, and DTMS (mass ratio = 100:2.8:1.2:0.4:1:2) were added to a beaker, mixed evenly, and then alumina (mean size 20 μm , 5 μm , and 2 μm , respectively; mass ratio = 7:1:2) were blended in a biplanetary vacuum mixer with a rotation speed of 40 rpm for 90 min to obtain Al_2O_3 /SR fluid (mass ratio of alumina to all oil and additives: 8.0). TCSR-based ultra-thin sheets were prepared on a calender. Glass fabric was sandwiched between two PET films, and the Al_2O_3 /SR fluid was put between the underlying PET films and glass fabric (Figure 1). The Al_2O_3 /SR fluid and glass fabric were pressed into liquid sheets on a double-roll calender (gap 0.20 mm) by the traction of the PET films and the inward rotation of the rolls. The liquid sheets were cured at 120 $^\circ\text{C}$ for 30 min in a tunnel furnace to obtain TCSR-based thin sheets. Their thickness was measured to be 0.15 mm with a vernier caliper (Figure 2b inset). They were thus labeled as 0.15 mm-thick sheets.

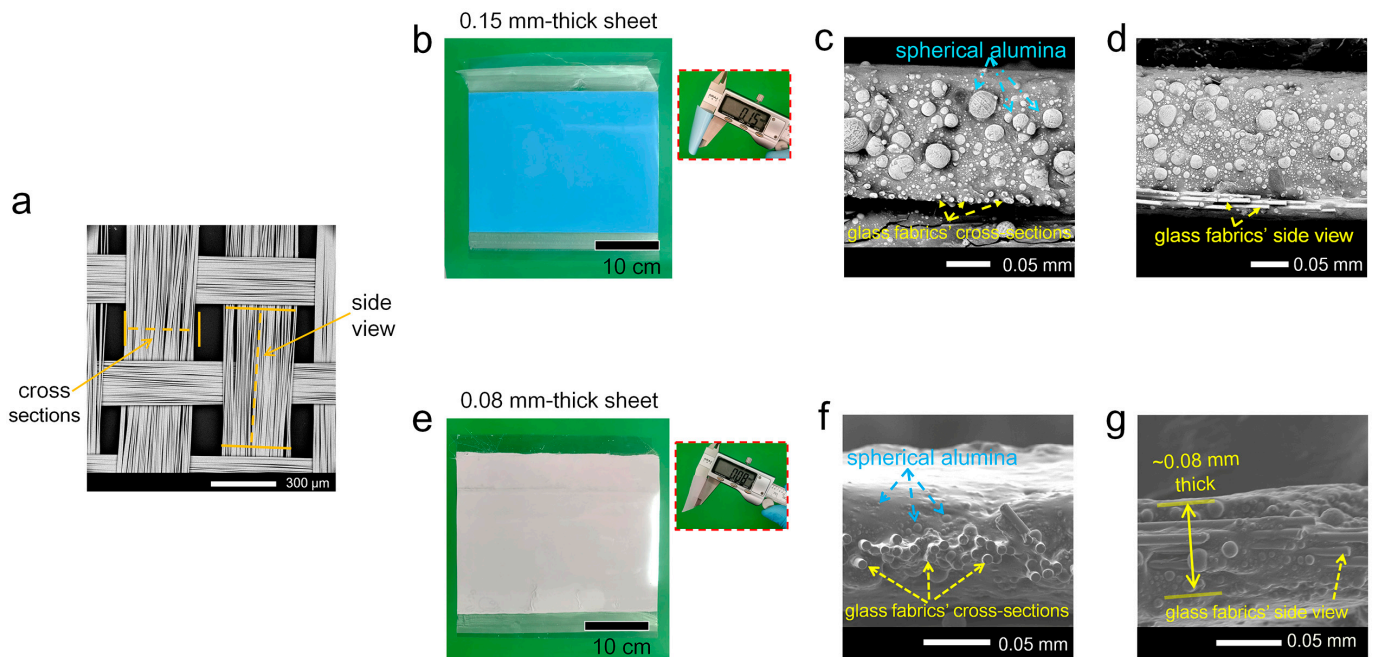


Figure 2. (a) SEM profile of glass fabric, and schematic diagram of the cross sections and side view of glass fabric. (b) Photograph of 0.15 mm-thick sheet prepared by the conventional method. (c) SEM profile of the 0.15 mm-thick sheet showing the cross sections of glass fabric. (d) SEM profile of the 0.15 mm-thick sheet showing the side view of glass fabric. (e) Photograph of 0.08 mm-thick sheet prepared by the low viscosity calendaring method. (f) SEM profile of the 0.08 mm-thick sheet showing the cross sections of glass fabric. (g) SEM profile of the 0.08 mm-thick sheet showing the side view of glass fabric.

2.3. Preparation of TCSR-Based Ultra-Thin Sheets by the Low Viscosity Method

A low-viscosity method was developed to produce TCSR-based ultra-thin sheets. In order to decrease the viscosity and flow resistance of the raw material fluids, low-viscosity vinyl silicone oil (100 mPa·s) and fine alumina (2–10 μm) were used.

The vinyl silicone oil, double-end-hydrogen silicone oil, side-hydrogen silicone oil, Pt catalyst, inhibitor, color masterbatch, DTMS (mass ratio = 100:18:1:1:0.3:1:3), 10 μm alumina, and 2 μm alumina (mass ratio = 7:3) were mixed to obtain Al_2O_3 /SR fluid (mass ratio of alumina to all oil and additives: 8.0). The fluid was made into TCSR-based thin sheets by the same method as in Section 2.2. The narrow gap on the calender was set as 0.15 mm. The sheets' thickness was measured to be 0.08 mm by Vernier calipers (Figure 2e). They were thus labeled as 0.08 mm-thick sheets.

2.4. Characterization

Glass fabric and sheet cross-sections were observed on a scanning electron microscope (SEM, Gemini SEM500, Zeiss, Germany). Tensile tests were run on a universal testing machine (AGS-X 50N, Suzhou Turbo Machinery Equipment Co. Ltd., Suzhou, Jiangsu Province, China). The electrical conductivity of the sheets was measured on an electrical resistance meter (FT-3204A, Ningbo Argal Instrument Co., Ltd., Ningbo, Zhejiang Province, China). The breaking voltage of the sheets was measured on an RK2671AM withstand voltage tester (Shenzhen Meric Electronic Technology Co. Ltd., Shenzhen, Guangdong Province, China) according to ASTM D 149. The thermal resistance of the sheets and other TIMS was measured on a thermally conductive instrument (DRL-III, Xiangtan Instrument & Meter Co. Ltd., Xiangtan, Hunan Province, China) according to ASTM D5470. Thermal dissipation tests were run on a home-made set-up consisting of a LED chip (power 10 W, ordered on Taobao.com, accessed on 10 September 2021), a heat sink (heat pipe radiator, ordered on Taobao.com, accessed on 10 September 2021), and an infrared camera (E8, FLIR Systems Inc., Wilsonville, OR, USA). Al_2O_3 /SR fluid viscosity was measured on an NDJ-79 viscosity meter (Shanghai Lichen Instrument Technology Co. Ltd., Shanghai, China).

3. Results and Discussions

3.1. Morphology

Figure 2 shows the morphology of the glass fabrics and typical TCSR-based thin sheets. The glass fabric has a mesh structure made of glass fiber. The mesh size (80–300 μm , Figure 2a) is large enough for the flow and penetration of Al_2O_3 /SR fluids. TCSR-based thin sheets have a sandwich-like structure consisting of glass fabric and thermally conductive silicone rubber (Figure 2c,d,f,g). Spherical alumina of various particle sizes is dispersed in a silicone rubber matrix homogeneously, and glass fabric is inserted in the composites. Figure 2c,d shows that the glass fabric is mostly located at one side of the 0.15 mm-thick sheets, while the glass fabric was mostly inserted in the middle of the 0.08 mm-thick sheets (Figure 2f,g). This is probably because the thermally conductive fillers in the 0.08 mm-thick sheets (mean size 10 μm) are smaller than those in the 0.15 mm-thick sheets (mean size of 20 μm), making it easier for Al_2O_3 /SR fluids to flow through the meshes on the glass fabric.

3.2. Mechanical and Electrical Insulation Properties

In practical applications, TCSR-based sheets are mostly operated by hand. The sheets' mechanical properties must be high enough to resist the forces in manual operation. A basic requirement of TCSR's mechanical properties is high softness (or low hardness). As a result, TCSRs mostly have low modulus and tensile strength (<1 MPa), particularly in those with high thermal conductivity. When the sheets are thick, they are still strong enough to resist the forces caused by manual operation. However, when the sheets are thin, the forces can easily deform or even destroy the sheets. Therefore, reinforcement materials are necessary for TCSR-based thin sheets, and glass fabric or polyimide (PI) films have been widely used as reinforcement materials.

The 0.15 mm-thick sheets and 0.08 mm-thick sheets both have high mechanical properties due to the incorporation of glass fiber. They can be twisted and recovered without any damage (Figure 3a,c), indicating high flexibility and toughness. Neat TCSR has a tensile strength of smaller than 0.30 MPa, and the tensile strength of the 0.15 mm-thick sheets and 0.08 mm-thick sheets is higher than 5 MPa (Figure 3b,d), which can be mainly attributed to the glass fiber in the sheets. It is interesting that the 0.08 mm-thick sheets have higher tensile strength than the 0.15 mm-thick sheets. This does not mean that the 0.08 mm-thick sheets can resist more force than the 0.15 mm-thick sheets. In fact, the two sheets can resist similar tensile force because the force is almost afforded by the glass fiber. Meanwhile, the 0.08 mm-thick sheets have a smaller thickness (or cross-section area) than the 0.15 mm-thick sheets. As a result, the tensile test results of the 0.08 mm-thick sheets present higher tensile strength than the 0.15 mm-thick sheets.

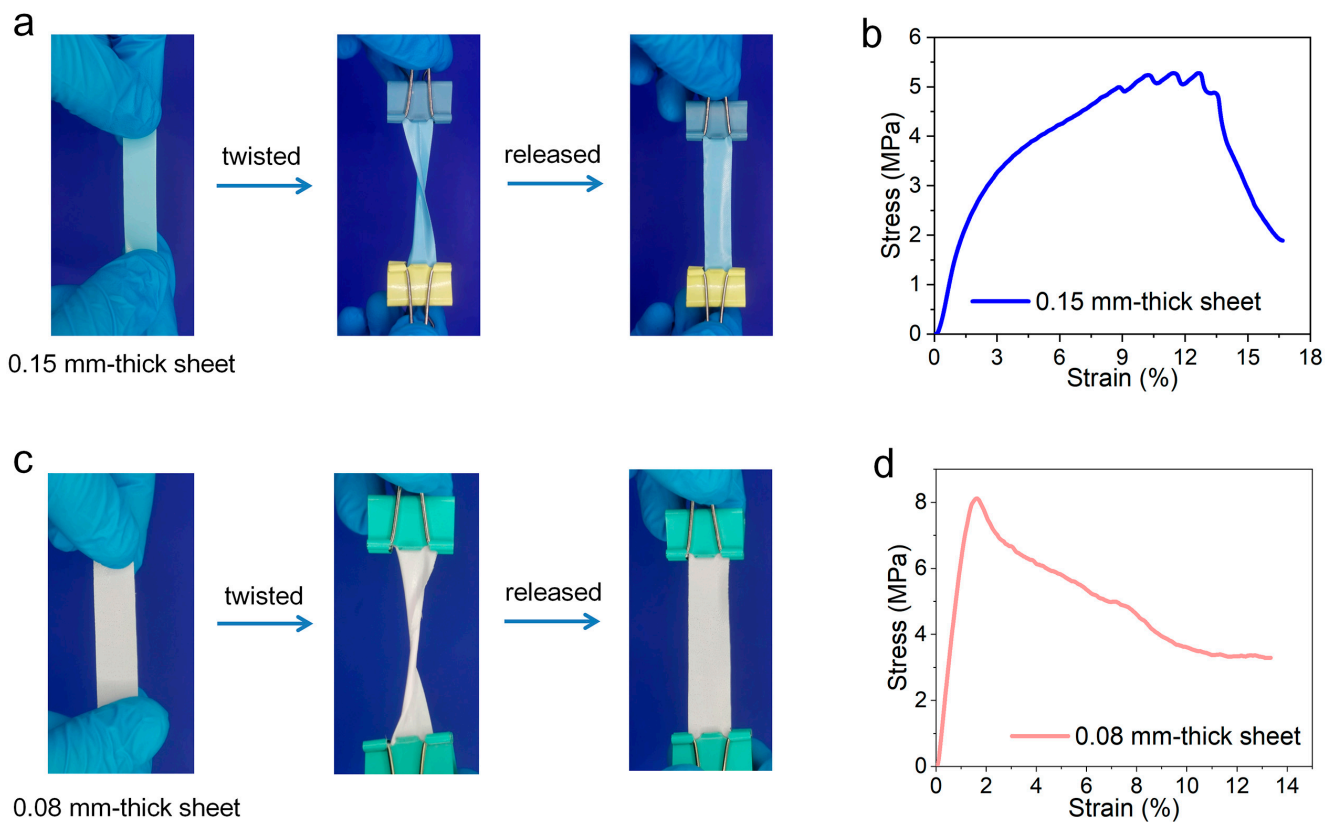


Figure 3. (a) Photographs showing the high flexibility of 0.15 mm-thick sheets prepared by the conventional method. (b) Typical tensile curve of 0.15 mm-thick sheets. (c) Photographs showing the high flexibility of 0.08 mm-thick sheets prepared by the low-viscosity calendering method; (d) Typical tensile curve of 0.08 mm-thick sheets.

Most applications of TCSR-based shin sheets require high electrical insulation properties, which are mainly evaluated by electrical resistance and breaking voltage. The 0.15 mm-thick sheets and 0.08 mm-thick sheets both have high electrical insulation properties. Their volume electrical conductivity is higher than $10^{14} \Omega \cdot \text{m}$ (beyond the test equipment's range), and their breaking strength is higher than 5.0 kV/mm. The high electrical insulation properties have been achieved because the raw materials, such as silicone oils, additives, alumina, and glass fabric, are all electrical insulators.

3.3. Thermal Properties

TIMs are usually put between heat sources and heat sinks to reduce the thermal resistance from the heat sources to the heat sinks. The total thermal resistance (R_{total}) includes three parts, as shown in Equation (1),

$$R_{\text{total}} = R_{\text{TIMs}} + R_{\text{-c1}} + R_{\text{-c2}} = \frac{t}{k} + R_{\text{-c1}} + R_{\text{-c2}} \quad (1)$$

where R_{TIMs} is the thermal resistance of the TIMs, $R_{\text{-c1}}$ and $R_{\text{-c2}}$ are the thermal resistance between the TIMs and the heat sources or heat sinks, t is the TIM thickness, and k is the TIM thermal conductivity.

Equation (1) suggests that the total thermal resistance is determined by the thermal resistance of the TIMs (R_{TIMs}) and the contacting state between the TIMs and the heat sources or sinks ($R_{\text{-c1}}$ and $R_{\text{-c2}}$). $R_{\text{-c1}}$ and $R_{\text{-c2}}$ are greatly affected by the softness (or hardness) of the TIMs. This is the main reason for the requirement of high softness or low hardness of TCSR sheets.

TIMs can be mainly classified into two types: (i) solid TIMs such as thermally conductive silicone rubber sheets and polyimide films; and (ii) liquid TIMs such as thermally conductive grease and liquid metal. Usually, liquid TIMs can be put between heat sources and heat sinks and pressed into a thin liquid film with a much smaller thickness (or BLT) than that of solid TIMs, and their liquid state affords good contact between the TIMs and the heat sources or heat sinks. As a result, liquid TIMs usually have much lower contacting thermal resistance than solid TIMs when they are tested in the same situation, even when the liquid TIMs have lower thermal conductivity than solid TIMs. This is a major advantage of liquid TIMs.

In order to better evaluate the effect of the low-viscosity calendaring method, we measured the thermal resistance of our TCSR-based thin sheets and typical electrically insulated TIMs on a thermal conductivity meter under the same conditions. In addition to the 0.15 mm-thick sheets and 0.08 mm-thick sheets, TIMs including Kapton PI film, thermally conductive silicone rubber pads with high thermal conductivity, and thermally conductive grease (X-23-7783D) were tested. The first three are solid TIMs, and the last is a famous liquid TIM widely used in the industry.

The test results are plotted against the TIMs' thickness to understand the relationship between the thermal resistance and the thickness (Figure 4). It is shown that the liquid TIMs X-23-7783D has much lower thermal resistance ($<1 \text{ cm}^2\text{K/W}$) than the conventional solid TIMs ($>2 \text{ cm}^2\text{K/W}$) and the 0.15 mm-thick sheet, while the 0.08 mm-thick sheet prepared by the low-viscosity calendaring method has obtained a thermal resistance ($0.87 \text{ cm}^2\text{K/W}$) almost as low as that of X-23-7783D. This thermal resistance is also lower than many PI-based thermally conductive sheets in the open literature [18,19]. The low thermal resistance of the 0.08 mm-thick sheet can be mainly attributed to its small thickness.

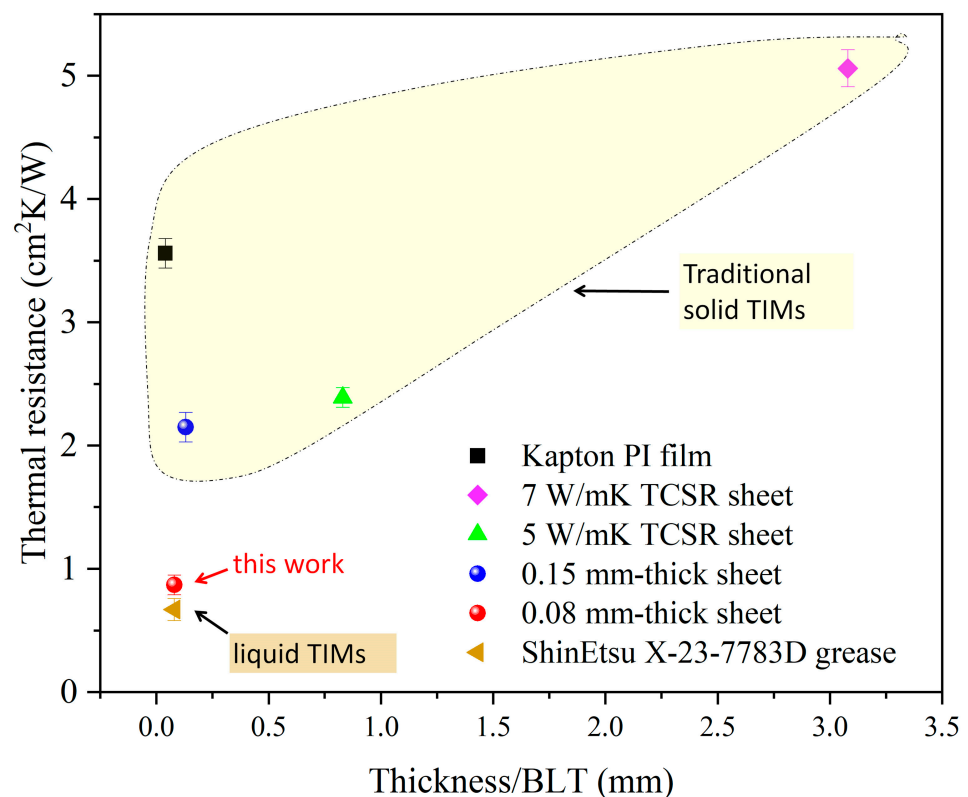


Figure 4. Scatter plots of the thermal resistance of typical electrically insulated TIMs against their thickness or BLT. The thickness and BLT here are the actual thickness during the thermal resistance tests. The 0.08 mm-thick TCSR-based sheet prepared by the low-viscosity calendaring method has a much lower thermal resistance than the conventional solid TIMs, comparable to that of high-performance thermal conductive grease X-23-7783D.

Due to the low thermal resistance, TCSR-based ultra-thin sheets can be used in thermal management applications. Here we evaluate its cooling performance on a homemade LED-based testing setup (Figure 5a). Comparison tests of a variety of TIMs were conducted. The infrared camera took infrared images at an ambient temperature of 30 °C. Figure 5b shows infrared images recording the working temperature on the LED chip. Figure 5c shows that the LED working temperature at 20 min was as high as 81.9 °C when there were no TIMs between the LED chip and the heat sink. When TIMs were placed between the LED chip and the heat sink, the LED working temperature decreased. The temperature was decreased to 51.7 °C when a 0.08 mm-thick sheet was used as the TIM. This cooling performance is comparable with that of ShinEtsu X-23-7783D thermally conductive grease and is better than that of the other solid TIMs tested. This is because the low thermal resistance of the 0.08 mm-thick sheet can effectively eliminate the intense heat generated by the LED.

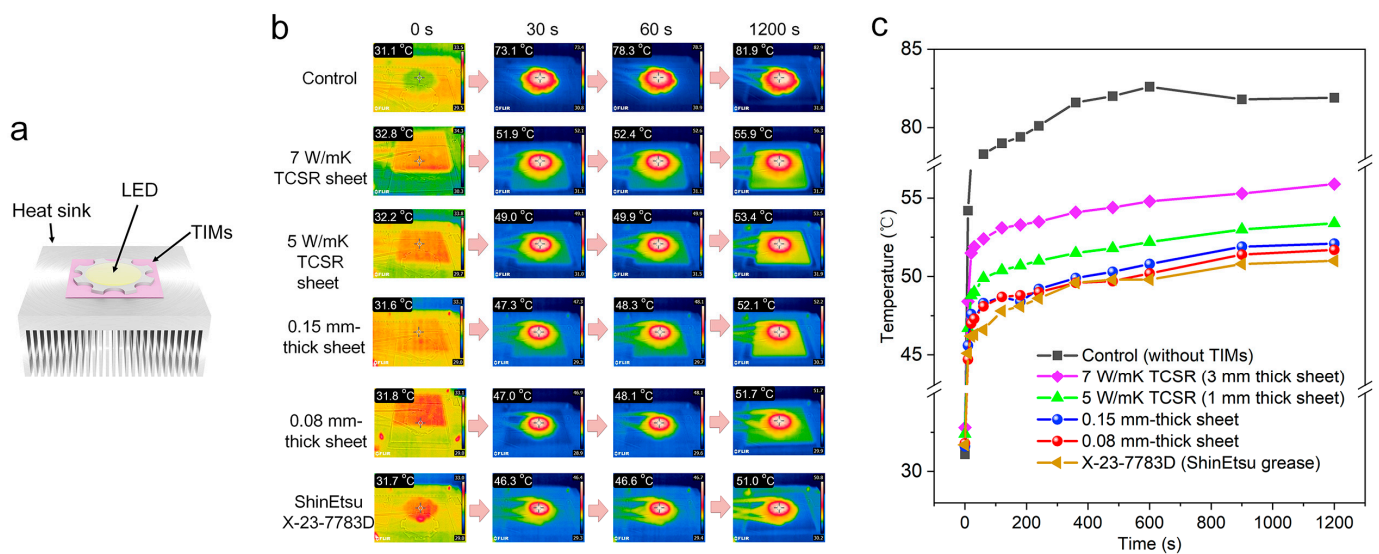


Figure 5. (a) Schematic diagram of the homemade setup for the cooling tests. (b) Typical infrared images showing the working temperature of the LED chips. (c) Plots of the working temperature of the LED chips with different TIMs against working time.

From the comparison of Figures 4 and 5c, it is clear that the lower the thermal resistance, the better the cooling performance. In particular, although the 7 W/mK thermally conductive silicone pad has the highest thermal conductivity, its cooling performance is the worst.

It is interesting to note that, although the 0.15 mm-thick sheet has higher thermal resistance than the 0.08 mm-thick sheet and the X-23-7783D grease, their cooling performance is close to each other. This is probably because of two reasons, (i) the working temperature was recorded with an infrared camera, which had limited accuracy; and (ii) the thermal resistance of the 0.15 mm-thick sheet is probably low enough to dissipate most of the heat, and, hence, a further decrease in thermal resistance does not contribute much to the cooling performance. It can be supposed that if the power of the LED chip was increased, the 0.08 mm-thick sheet and the X-23-7783D grease may present better cooling performance than the 0.15 mm-thick sheet due to their lower thermal resistance.

In addition, it should be also noted that the test results on thermal resistance and thermal dissipation performance are greatly affected by the test equipment and test conditions. For instance, if the load used in the thermal resistance tests is changed, the test results may present obvious changes. These problems will be studied in detail in another work.

4. Discussion

TCSR-based thin sheets' thickness is controlled by the narrow gap on the calender. When the gap is sufficiently small, it may become difficult to calender raw material fluids due to the increased flow resistance of the raw materials fluids.

Figure 6 presents the preparation process of TCSR-based thin sheets. Raw materials such as spherical Al_2O_3 , silicone oils, and additives were mixed homogeneously to form Al_2O_3 /SR fluids. The fluids were pressed into thin sheets on a double-roller calender, followed by heat curing to obtain solid thin sheets. The sheets were protected by two PET films (release films). Glass fabric was blended into the thin sheets for mechanical strengthening.

The Al_2O_3 /SR fluids have high viscosity due to the high loading level of Al_2O_3 in the fluids. The high viscosity may bring large resistance when the Al_2O_3 /SR fluids flow across the narrow gap. Due to the high viscosity, some fluids may deposit in front of the rollers, as shown in Figure 6a. These deposited zones may bring a further increase in flow resistance. The high flow resistance has a negative impact on the calendaring process.

Besides the viscosity, the size of the alumina particles also has a great impact on the resistance. As illustrated in Figure 6b, there are two PET films and a glass fabric film in the narrow gap, and the space for moving alumina particles across the gap is actually less than 50 μm . When the diameter of the alumina particles is large, it will be difficult for the particles to move in the small space between the PET films and glass fabric, bringing large flow resistance to Al_2O_3 /SR fluids.

Based on the above consideration, in order to obtain TCSR-based ultra-thin sheets, we made two optimizations to reduce the flow resistance of Al_2O_3 /SR fluids across the narrow gap: (i) reducing the Al_2O_3 /SR fluids' viscosity by using silicone oil with low viscosity; and (ii) reducing the size of the alumina particles.

Figure 6c,d shows the effects of the optimization. Two Al_2O_3 /SR fluids were prepared. One was prepared from the most typical raw materials in the industry and by the most conventional method used currently. The vinyl silicone oil had a viscosity of about 500 mPa·s at 25 °C, and the major thermally conductive filler was spherical alumina with a mean size of 20 μm . After the raw materials were mixed together, the resultant Al_2O_3 /SR fluid had a viscosity of about 143 Pa·s. The fluids were calendered and heat-cured to obtain TCSR-based thin sheets. Various gap sizes were studied. The smallest gap that could obtain smooth sheets was 0.20 mm, and the obtained sheets had a thickness of about 0.15 mm (seeing Figure 2b inset). When the gap was decreased to 0.18 mm, the resultant sheets were deformed, as shown in Figure 6c.

Another Al_2O_3 /SR fluid was prepared from low-viscosity vinyl silicone oil (100 mPa·s) and fine spherical alumina powder (mean size of 10 μm), etc. The fluid had a viscosity of about 86 Pa·s. It could be successfully calendered when the gap was only 0.15 mm in width. The obtained sheets had a thickness of about 0.08 mm (seeing Figure 2e inset). When the gap was set as 0.13 mm, the fluid could not be calendered into smooth sheet (Figure 2d).

Overall, the calendaring process of Al_2O_3 /SR fluid or similar raw material mixtures is actually a hydrodynamics problem occurring in a narrow gap. Based on this study, it can be confirmed that the thickness of TCSR-based thin sheets can be successfully decreased by the low-viscosity calendaring method, and the use of low-viscosity silicone oil and fine alumina powder is the main cause of the successful calendaring.

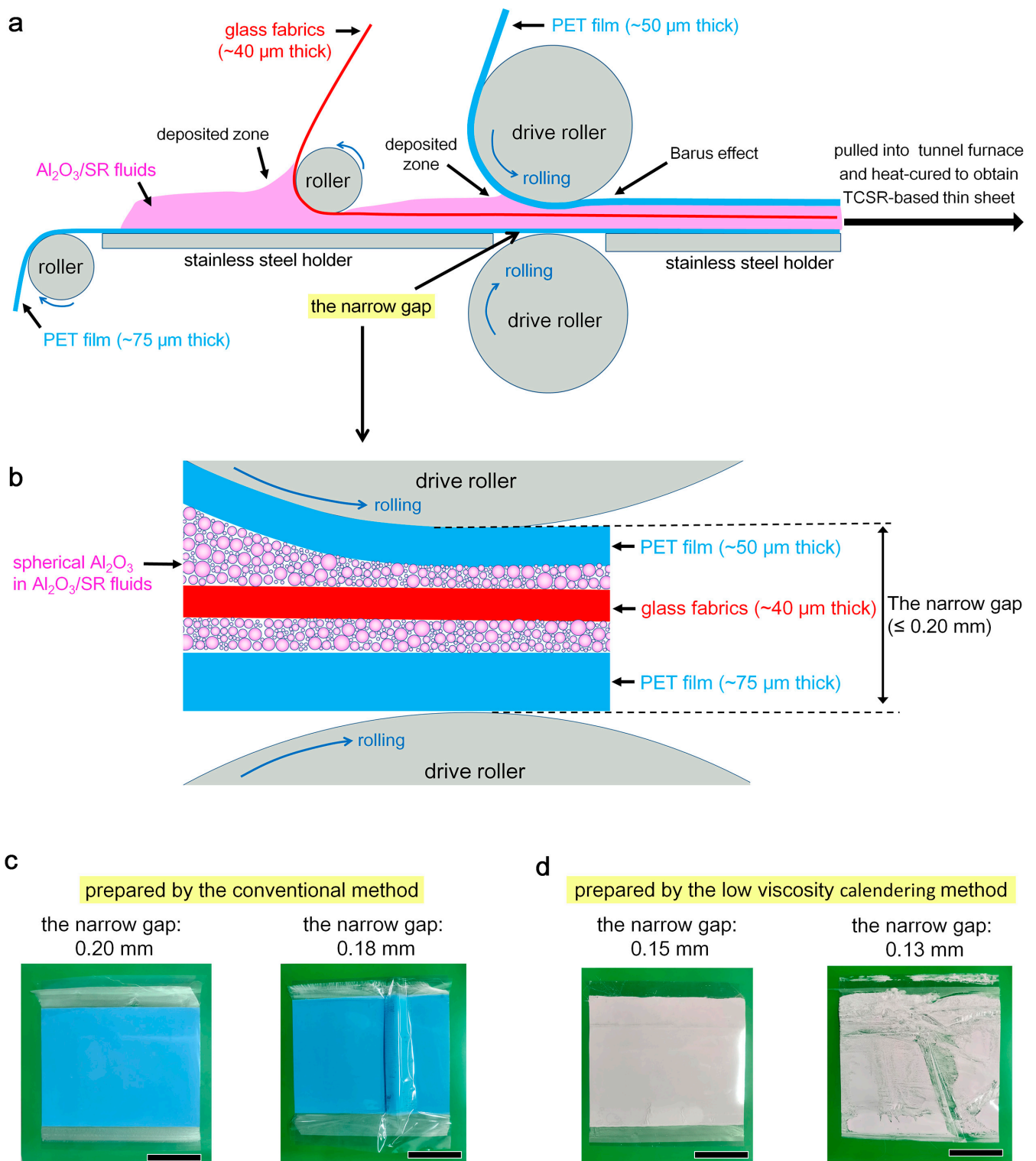


Figure 6. (a) Schematic diagram of the calendaring process of Al₂O₃/SR fluids; (b) Schematic diagram of the narrow gap where alumina particles are forced to move and cross; (c) Photos showing TCSR-based thin sheets prepared by the conventional method with different narrow gaps; (d) Photos showing TCSR-based ultra-thin sheets prepared by the low-viscosity calendaring method.

5. Conclusions

Thermally conductive silicone rubber-based ultra-thin sheets have been successfully prepared from fine spherical alumina powder and low-viscosity silicone oil by a low-viscosity calendering method. Compared with similar thin sheets prepared by the conventional method, the ultra-thin sheets have an unprecedentedly small thickness (~0.08 mm), high strength (~8 MPa), high flexibility, high electrical resistance ($>10^{14}$ $\Omega\cdot\text{cm}$), high breaking strength (~5.3 kV), low thermal resistance (0.87 $\text{cm}^2\text{K/W}$), and high thermal dissipation (>30 °C decrease in LED working temperature). Comparison studies on the calendering process suggest that the low viscosity of the raw material fluid is the key factor for successful preparation. The proposed approach could provide an effective and promising route to the development of high-performance thermally conductive silicone rubber and ultra-thin sheets for thermal management applications.

Author Contributions: Conceptualization, M.L. and C.B.; methodology, M.L. and J.L.; investigation, M.L. and X.G.; resources, S.T. and C.B.; writing—original draft preparation, M.L.; writing—review and editing, J.Y., J.L. and C.B.; supervision, C.B.; funding acquisition, C.B. All authors have read and agreed to the published version of the manuscript.

Funding: This research received no external funding.

Data Availability Statement: Data supporting reported results can be obtained from C.B. through email.

Acknowledgments: This work was supported by the R&D programs of Tianjin Haite Thermal Management Technology, Co., Ltd., Tianjin, China. (No. 2301/029175) and Sichuan Ximaiwan Technology Co., Ltd., Chengdu, Sichuan Province, China.(No. 2301/029514).

Conflicts of Interest: The authors declare no conflict of interest.

References

1. Zhang, X.; Li, Z.; Luo, L.; Fan, Y.; Du, Z.Y. A review on thermal management of lithium-ion batteries for electric vehicles. *Energy* **2022**, *238*, 121652. [[CrossRef](#)]
2. Ma, H.Q.; Gao, B.; Wang, M.Y.; Yuan, Z.Y.; Shen, J.B.; Zhao, J.Q.; Feng, Y. Strategies for enhancing thermal conductivity of polymer-based thermal interface materials: A review. *J. Mater. Sci.* **2021**, *56*, 1064–1086. [[CrossRef](#)]
3. Zhang, Y.; Hao, N.; Lin, X.; Nie, S. Emerging challenges in the thermal management of cellulose nanofibril-based supercapacitors, lithium-ion batteries and solar cells: A review. *Carbohydr. Polym.* **2020**, *234*, 115888. [[CrossRef](#)] [[PubMed](#)]
4. Zhang, Y.F.; Han, D.; Zhao, Y.H.; Bai, S.L. High-performance thermal interface materials consisting of vertically aligned graphene film and polymer. *Carbon* **2016**, *109*, 552–557. [[CrossRef](#)]
5. Teng, W.Y.; Tseng, H.M.; Hung, L.Y.; Wang, Y.P. High performance film-type thermal interface material containing vertically aligned carbon nanofibers. In Proceedings of the 20th International Conference on Electronics Packaging (ICEP), Electr Network, Tokyo, Japan, 12–14 May 2021; pp. 141–142.
6. Huang, J.Z.; E, S.; Li, J.Y.; Jia, F.F.; Ma, Q.; Hua, L.; Lu, Z. Ball-milling exfoliation of hexagonal boron nitride in viscous hydroxyethyl cellulose for producing nanosheet films as thermal interface materials. *ACS Appl. Nano Mater.* **2021**, *4*, 13167–13175. [[CrossRef](#)]
7. Song, Q.; Zhu, W.; Deng, Y.; Hai, F.; Wang, Y.; Guo, Z.P. Enhanced through-plane thermal conductivity and high electrical insulation of flexible composite films with aligned boron nitride for thermal interface material. *Compos. Part A-Appl. Sci. Manuf.* **2019**, *127*, 105654. [[CrossRef](#)]
8. Lv, L.; Dai, W.H.; Yu, J.; Jiang, N.; Lin, C.T. A mini review: Application of graphene paper in thermal interface materials. *New Carbon Mater.* **2021**, *36*, 930–938. [[CrossRef](#)]
9. Liu, H.B.; Su, X.Q.; Fu, R.L.; Wu, B.Y.; Chen, X.D. The flexible film of SCF/BN/PDMS composites with high thermal conductivity and electrical insulation. *Compos. Commun.* **2021**, *23*, 100573. [[CrossRef](#)]
10. Liu, H.; Fu, R.; Su, X.; Wu, B.; Wang, H.; Xu, Y.; Liu, X. Electrical insulating MXene/PDMS/BN composite with enhanced thermal conductivity for electromagnetic shielding application. *Compos. Commun.* **2021**, *23*, 100953. [[CrossRef](#)]
11. Zhang, Y.Y.; Ma, J.; Wei, N.; Yang, J.; Pei, Q.X. Recent progress in the development of thermal interface materials: A review. *Phys. Chem. Chem. Phys.* **2021**, *23*, 753–776. [[CrossRef](#)] [[PubMed](#)]
12. Yuan, Z.Y.; Ma, H.Q.; Hussien, M.A.; Feng, Y.K. Development and challenges of thermal interface materials: A review. *Macromol. Mater. Eng.* **2021**, *306*, 2100428. [[CrossRef](#)]
13. Bahru, R.; Zamri, M.F.M.A.; Shamsuddin, A.H.; Shaari, N.; Mohamed, M.A. A review of thermal interface material fabrication method toward enhancing heat dissipation. *Int. J. Energy Res.* **2021**, *45*, 3548–3568. [[CrossRef](#)]

14. Hansson, J.; Zanden, C.; Ye, L.; Liu, J. Review of current progress of thermal interface materials for electronics thermal management applications. In Proceedings of the 16th IEEE International Conference on Nanotechnology (IEEE-NANO), IEEE Nanotechnol Council, Sendai, Japan, 22–25 August 2016; pp. 371–374.
15. Khan, J.; Momin, S.A.; Mariatti, M. A review on advanced carbon-based thermal interface materials for electronic devices. *Carbon* **2020**, *168*, 65–112. [[CrossRef](#)]
16. Feng, C.-P.; Yang, L.-Y.; Yang, J.; Bai, L.; Bao, R.-Y.; Liu, Z.-Y.; Yang, M.-B.; Lan, H.-B.; Yang, W. Recent advances in polymer-based thermal interface materials for thermal management: A mini-review. *Compos. Commun.* **2020**, *22*, 100528. [[CrossRef](#)]
17. Guo, Y.; Ruan, K.; Shi, X.; Yang, X.; Gu, J. Factors affecting thermal conductivities of the polymers and polymer composites: A review. *Compos. Sci. Technol.* **2020**, *193*, 108134. [[CrossRef](#)]
18. Zhao, L.; Phelan, P. Thermal contact conductance across filled polyimide films at cryogenic temperatures. *Cryogenics* **1999**, *39*, 803–809. [[CrossRef](#)]
19. Ruan, K.; Guo, Y.; Lu, C.; Shi, X.; Ma, T.; Zhang, Y.; Kong, J.; Gu, J. Significant reduction of interfacial thermal resistance and phonon scattering in graphene/polyimide thermally conductive composite films for thermal management. *Research* **2021**, *2021*, 8438614. [[CrossRef](#)] [[PubMed](#)]

Disclaimer/Publisher’s Note: The statements, opinions and data contained in all publications are solely those of the individual author(s) and contributor(s) and not of MDPI and/or the editor(s). MDPI and/or the editor(s) disclaim responsibility for any injury to people or property resulting from any ideas, methods, instructions or products referred to in the content.